Distributed Phased Arrays: Challenges and Recent Advances

Jeffrey A. Nanzer, *Senior Member, IEEE*, Serge R. Mghabghab, *Graduate Student Member, IEEE*, Sean M. Ellison, *Member, IEEE*, and Anton Schlegel, *Graduate Student Member, IEEE*

***Abstract*— There has been significant research devoted to the development of distributed microwave wireless systems in recent years. The progression from large, single-platform wireless systems to collections of smaller, coordinated systems on separate platforms enables significant benefits for radar, remote sensing, communications, and other applications. The ultimate level of coordination between platforms is at the wavelength level, where separate platforms operate as a coherent distributed system. Wireless coherent distributed systems operate in essence as distributed phased arrays, and the signal gains that can be achieved scale proportionally to the number of transmitters squared multiplied by the number of receivers, providing potentially dramatic increases in wireless system capabilities enabled by increasing the number of nodes in the array. Coordinating the operations of nodes in a distributed array requires accurate control of the relative electrical states of the nodes. The basic challenge is the synchronization and stability of the relative phases of the signals transmitted or received. Generally, such control requires wireless frequency synchronization, phase calibration, and time alignment. For radar operations, phase control also requires high-accuracy knowledge of the relative positions of the nodes in the array to support beamforming. Various technologies have been developed in recent years to address the coordination challenges for closed-loop applications, such as distributed communications, and more recently, there has been growing interest in new technologies for open-loop applications, such as radar and remote sensing. This article presents an overview of distributed phased arrays, the principal challenges involved in their coordination, and recent research progress addressing these challenges.**

***Index Terms*— Distributed arrays, distributed beamforming, phased arrays, radar, remote sensing.**

I. Introduction

WIRELESS technologies supporting communication between separate wireless systems have advanced dramatically in recent years, enabling distributed cooperation of separate systems at previously unachievable levels. While information sharing has long been of interest for distributed applications such as wireless sensor networks [1], [2], distributed automotive radar [3], [4], and multiple-input–multiple-output (MIMO) radar [5], [6], recently there has been increasing interest in coordinating separate systems at a more granular scale. The ultimate level of cooperation between systems is at the scale of the wavelength of the wireless operation, where individual wireless nodes in a distributed array transmit and/or receive signals coherently, forming a distributed phased array. Coordinating systems at the wavelength level provides an alternative to the platform-centric paradigm currently dominating wireless system development: for most wireless systems, improving performance entails redesigning or retrofitting existing large or single-platform systems, whether large radar systems or hand-held wireless devices; in contrast, by disaggregating the functionality of a single platform into a distributed network of small, wireless nodes (see Fig. 1), a coherent distributed system can achieve performance improvements by simply adding more low-cost nodes to the array. Distributed phased arrays, or coherent distributed antenna arrays, consist of a number of separate wireless nodes that transmit signals coherently to enable beamforming and/or coprocess received signals coherently to form beams on receive digitally. Single-platform phased arrays traditionally use analog feed networks to distributed signals between the antenna elements and a single centralized transceiver [7], [8]. In contrast, distributed arrays operate similar to element-level digital phased arrays, where each antenna element is connected to a separate transceiver [9], [10]. Accurately controlling the phase states of the individual nodes in a distributed array enables distributed beamforming, from which a range of benefits is afforded, including the following.

1) *Enhanced Signal Gain:* An array of N transmitters yields N^2 signal gain at the destination from the aggregate signal power and directivity from beamforming, while a gain of M is obtained from M receivers from beamforming; the distributed phased array gain, thus, scales as N^2M, yielding improved signal-to-noise ratio (SNR).
2) *Increased Reliability:* Multiple nodes cooperating coherently can remove single-point-of-failure; if a node fails or suffers interference, the distributed array operation degrades gracefully.
3) *Scalability:* Increases in signal gain can be achieved directly by including more nodes in the array.

Manuscript received February 26, 2021; revised May 8, 2021; accepted May 29, 2021. Date of publication July 21, 2021; date of current version November 4, 2021. This work was supported in part by the Defense Advanced Research Projects Agency under Grant N66001-17-1-4045, in part by the Office of Naval Research under Grant N00014-17-1-2886, and in part by the National Science Foundation under Grant 1751655. *(Corresponding author: Jeffrey A. Nanzer.)*

Jeffrey A. Nanzer, Serge R. Mghabghab, and Anton Schlegel are with the Department of Electrical and Computer Engineering, Michigan State University, East Lansing, MI 48824 USA (e-mail: nanzer@msu.edu; mghabgha@msu.edu; schleg19@msu.edu).

Sean M. Ellison was with the Department of Electrical and Computer Engineering, Michigan State University, East Lansing, MI 48824 USA. He is now with the Johns Hopkins University Applied Physics Laboratory, Laurel, MD 20723 USA (e-mail: elliso65@msu.edu).

Color versions of one or more figures in this article are available at https://doi.org/10.1109/TMTT.2021.3092401.

Digital Object Identifier 10.1109/TMTT.2021.3092401

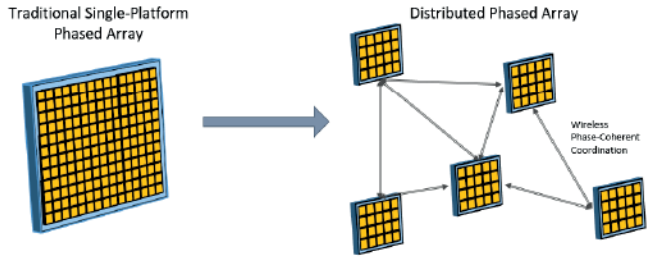

Fig. 1. Distributed phased arrays overcome the limitations of platform-centric wireless system models by disaggregating the functionality of large wireless systems into an array of smaller, cheaper nodes that are wirelessly coordinated to support distributed beamforming.

4) *Adaptability:* Nodes may be reallocated in space to adapt to changing conditions; the array may separate into multiple smaller distributed arrays to perform multiple functions.
5) *Greater Spatial Diversity:* Increasing the array size yields narrower directed beams and greater spatial resolution.

There are additional benefits that may manifest, e.g., cost benefits in launching a set of small satellites as opposed to a single large satellite; nevertheless, these additional benefits tend to be more application-specific. To obtain these and other benefits, the electrical states of the individual nodes in the array must be accurately synchronized. However, achieving the necessary level of synchronization between nodes that are physically separated and that may be in relative motion is a challenging task. Not only must the internal electronics, such as local oscillators, be synchronized wirelessly but also the movement of the nodes themselves must be addressed. Global navigation satellite systems (GNSS), such as the global positioning system (GPS), provide synchronization capabilities that are far too coarse in position, frequency, and time to support phase coherence at microwave frequencies. Hence, the coordination tasks must be accomplished within the distributed array itself.

A growing body of research has focused on the use of feedback from a wireless system that is collocated with the beamforming destination or, more commonly, is the intended beamforming destination itself [11]–[14]. For example, a set of wireless communication systems connected to a base station can receive feedback from the base station regarding the received signal strength, from which the nodes can adjust their states until beneficial signal strength is achieved. This closed-loop approach has a number of benefits, namely, little coordination between the nodes in the array needs to be implemented; for example, the precise locations of the nodes need not be known. Such an approach is feasible for communications applications, where the beamforming destination is a wireless system itself, but is not applicable to sensing applications, such as radar, where feedback from the destination, if present at all, is a result of the target scattering characteristics and, in practice, is not feasible to use in determining the precise beamforming state of the array. Closed-loop systems, furthermore, can only beamform to the location providing the feedback, with no feasible direct mechanism to then steer a beam to a different, arbitrary angle.

Phased array technology has yielded dramatic benefits for wireless applications in general, not only for communications [15], [16]. Radar systems, which must overcome the more dramatic R^{-4} propagation losses compared to the R^{-2} losses in one-way communications systems, have increasingly relied on beamforming to achieve greater SNR and better directivity. Achieving greater signal gain in phased arrays has motivated research on component and device technologies, such as more efficient amplifiers and larger antenna apertures, but achieving capability improvements through component or aperture redesign is an increasingly challenging task that can potentially be addressed in a more cost-effective and rapid manner if separate small apertures can be coherently combined. Remote sensing applications, whether active or passive, generally benefit from improved spatial resolution, for instance, in satellite remote sensing of the earth. Increasing aperture sizes is a considerable challenge for satellite systems that can be addressed by coherently combining the apertures on small satellites that can more easily be deployed and replaced. In general, coherent distributed sensing systems must be designed as open-loop arrays such that there is no reliance on feedback from the destination; the array must self-align the electrical states of the nodes, thereby allowing beamsteering to arbitrary angles, and the potential for any wireless application.

Achieving open-loop distributed beamforming is a considerably more challenging task than the closed-loop approach and involves a compounding number of potential errors that must be characterized and mitigated or controlled. However, recent research has begun to demonstrate solutions to the most fundamental challenges involved in open-loop distributed beamforming, which has opened the door for expanded investment in applied distributed phased array research. Many of these solutions are based on microwave system design or codesign with signal processing, particularly analog wireless frequency synchronization and high-accuracy internode ranging. This article discusses recent developments in distributed phased research, including synchronization requirements, recent technical developments, and experimental demonstrations. While many applications can be categorized as either closed-loop or open-loop, it is anticipated that there will be situations where techniques applying to both approaches will be useful; as such, this article discusses recent results of both types of systems. The focus of this article is on the microwave technologies supporting phase-coherent coordination between separate nodes for distributed beamforming and does not discuss the implications of the resultant beam patterns of such distributed systems. Due to their inherently sparse nature, distributed phased array beam patterns generally manifest with a large number of grating lobes, which may be relevant for a given application and can be approached with various array design methods [17]–[20]. This article is organized as follows. In Section II, the closed- and open-loop topologies are discussed in more detail, followed by a detailed discussion of the principal coordination challenges faced in distributed phased array design in Section III. Recent developments addressing the principal coordination challenges are reviewed in Section IV, followed by recent proof-of-concept experimental

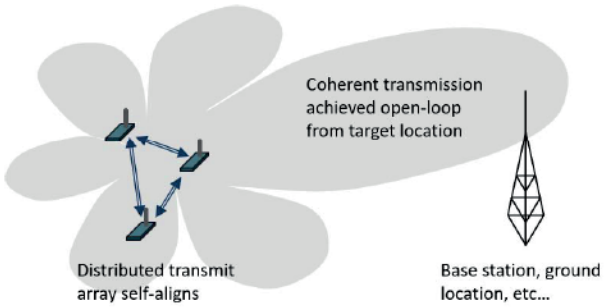

Fig. 2. Open-loop distributed phased arrays achieve distributed beamforming through internode synchronization of the nodes in the array without external signaling. Coordination between the nodes is challenging, but the open-loop architecture enables beamforming to arbitrary angles, thus supporting any wireless operation.

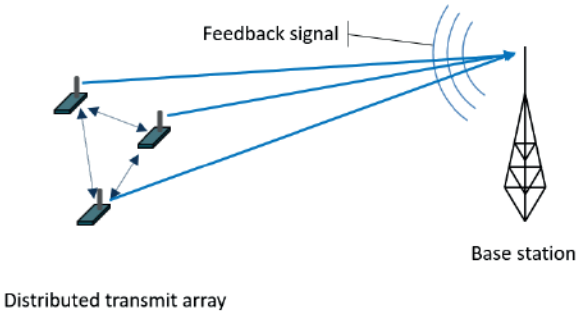

Fig. 3. Closed-loop distributed beamforming systems utilize feedback from the destination system to adjust the electrical states of the nodes until a high-gain state is obtained. Closed-loop beamforming can be accomplished with little to no coordination between the nodes, but the operation can only beamform to the receiving system and cannot arbitrarily steer beams.

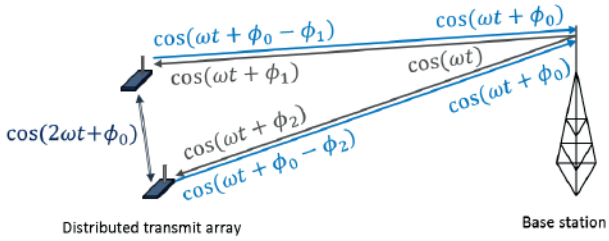

Fig. 4. Retrodirective distributed beamforming arrays utilize signals emitted by the destination system. If frequency synchronized and time-aligned, retrodirective approaches, such as a Pon array [22], can be implemented. The phase delays from the emitter (base station) to each node ϕ_i are mixed with twice the carrier frequency, yielding retransmitted carrier signals whose phase cancels the propagation phase delay, yielding phase-coherent signal summation at the emitter. Similar to the closed-loop architecture, the operation can only beamform to the receiving system.

distributed beamforming systems in Section V. This article concludes with a summary of the remaining challenges.

II. Distributed Phased Array Coordination Architectures

Distributed phased arrays can generally be categorized into open- and closed-loop systems. In open-loop architectures, nodes within the distributed array align their electrical states relative to one another and form beams to desired directions *without relying on feedback from the destination* to achieve phase coherence (see Fig. 2) [21]. The destination may be an active system, such as a base station, (for example, the aggregated signal gain of the array can be used to close a link when individual nodes do not have sufficient SNR to do so individually) or the destination may be a location on the ground in the case of a remote sensing operation. Open-loop systems are, therefore, not constrained by spatial location or feedback signals; they are flexible and could be used in a dynamic setting as long as sufficient synchronization within the array is achieved. Open-loop architectures support any general wireless operation, but this flexibility comes at the cost of significant coordination requirements, as discussed further in Section III; among the major challenges are accurately estimating the internode range and wirelessly synchronizing the oscillators on each node.

Closed-loop distributed beamforming relies on a signal from the destination and can be subcategorized as feedback-enabled or retrodirective distributed beamforming. Many techniques that support coherent beamforming in a closed-loop setting have been developed in the literature; among these approaches, coherent operation was supported using primary-secondary synchronization [11], receiver-coordinated explicit-feedback [23], one-bit feed back [24], roundtrip synchronization [25], and two-way synchronization [26].

A feedback-enabled closed-loop architecture relies on external inputs from the targeted location in order to enable coherence (see Fig. 3). Commonly, minimal to no coordination is required between the array nodes; the feedback from the targeted base station is used to synchronize the frequency, time, or phase on the individual nodes to achieve a phase-coherent beam at the destination. The feedback is commonly dependent on the received power level, and phase or time adjustments are implemented in the nodes to maximize the power level. Convergence to a high-gain state is generally inversely dependent on the amount of information shared between nodes and the amount of information provided as feedback from the destination node. As little as one bit of feedback from the target node is sufficient to support beamforming [24], however, the convergence time may be above that of the coherence length of the channels in mobile nodes. As noted above, current feedback-enabled beamforming methods only reliably cohere the transmitted signals at the destination and do not allow for controlled beamforming to other directions.

Retrodirective beamforming arrays are a form of closed-loop architecture where the array uses an external signal in order to achieve coherent operation, but the received signal need not be cooperative [22], [27]–[29]. Reciprocity is used by the nodes to adjust their channel gains or frequency by analyzing incoming signals from the base station or external sensors without having any cooperative communication with the external sources, which can offset intrinsic phase delays in each channel (see Fig. 4), operating like a Pon array [22]. As an example, the base station can broadcast a strong signal that can be used by every individual node in the array to adjust the frequency of its oscillator. Like the closed-loop architecture, the retrodirective architecture can achieve coherent signal summation only at the emitting system and cannot beamform to other specific angles.

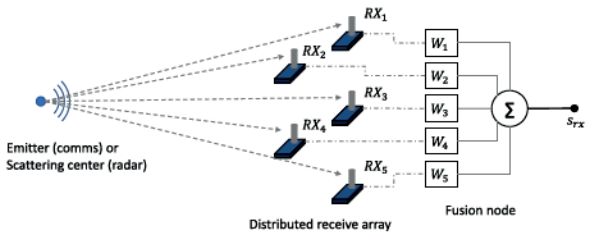

Fig. 5. Open-loop distributed receive beamforming architecture. A set of receivers with only frequency synchronization capture signals emitted or scattered from a remote point. The signals are combined in a fusion node by weighting the received signals in an optimized approach to maximize the beamforming gain. The fusion node may reside within or outside the distributed array.

The function of the distributed phased array—whether it is intended to transmit, receive, or both—can impact the architecture. Distributed receive beamforming is a specific subset of distributed beamforming that focuses on the ability of a distributed array to coprocess wireless signals from a distant transmitter to improve signal quality in some form. In distributed receive beamforming, the elements are physically separated and coordinated at the level of the RF phase wirelessly. The signals are digitized and transmitted to a processing node, which may or may not reside within the array, as shown in Fig. 5. In contrast to amplify-and-forward beamforming approaches where feedback from the transmitter is used in the optimization process [30]–[32], distributed reception generally assumes that the distributed receive array obtains beamforming gain without feedback from the transmitter. The fusion node applies optimization to obtain a coherent summation of the separate received signals. Various approaches have been investigated. In [33] and [34], phase correction via feedback from the fusion node was investigated; this approach, however, requires additional wireless communications between nodes. Various methods have been investigated for reducing wireless throughput between nodes in the receive array. In [35], distributed processing of hard decisions, where bits are individually decoded and forwarded, was shown to result in beamforming degradation of less than 2 dB. While applicable to communications, this approach is nonetheless not generalizable to all wireless operations, such as radar and remote sensing. Other methods have explored amplify-and-forward approaches using coded waveforms; however, these generally presume existing knowledge of the channel state [36], [37].

III. Coherent Distributed Coordination: Principal Challenges in Distributed Phase Synchronization

The objective of a distributed beamforming operation is to ensure that emitted signals arrive at the desired destination in-phase and with sufficient relative timing such that the signals add in the desired way (usually constructively to increase signal power), or if receiving signals, to ensure that the relative phase and timing of the received signals are aligned so that coherent coprocessing can take place. The methods by which the relative phases and times are estimated and corrected differ based on whether the system is only receiving signals or whether the system must transmit. In the former, data-driven approaches where, for example, the phases of the received signals are estimated and corrected in postprocessing, may be implemented at the cost of latency. Coherent distributed transmission is a significantly harder challenge since the relative electrical states of the antennas in the distributed array must be aligned *in situ* and often in real time. This entails ensuring that all nodes are operating at the same frequency, phase errors due to internal subsystem delays are calibrated, and phase and timing differences due to the relative locations of the nodes are estimated and corrected. In this section, we describe the principal factors impacting distributed coherence and the accuracy to which they must be estimated and corrected to ensure a high level of coherent operation. The analysis describes a transmit operation since it represents a more challenging implementation; however, the error terms and the resulting required estimation accuracies are valid for transmit or receive operations.

A. Distributed Beamforming Model

In an ideal distributed beamforming operation, the transmitted signals from the N nodes in the array arrive at the destination at the same time, with the same frequency and phase, and with channel imbalances corrected. The ideal received signal is

$$s_i(t) = \sum_{n=1}^{N} A_n(t) e^{j2\pi f_c t} \tag{1}$$

where $A_n(t)$ is the complex baseband signal, which is generally time-varying (e.g., a radar pulse or a communications symbol), and f_c is the carrier frequency. In practice, the received signal in the far-field of an array of N arbitrarily placed transmitting nodes can be represented by

$$s_r(t) = \sum_{n=1}^{N} h_n A_n(t - \delta t_n) e^{j(2\pi f_c t + \delta\psi_n)} \tag{2}$$

where $h_n = \alpha_n e^{j\phi_n^{(h)}}$ is the complex-valued coefficient representing the propagation channel from transmitter n to the destination, δt_n represents the timing difference between the transmitted signals, and $\delta\psi_n$ is the total phase difference, which can be given by $\delta\psi_n = 2\pi\delta f_n t + \delta\phi_n^{(s)} + \delta\phi_n^{(c)}$, where $2\pi\delta f_n t$ is the instantaneous phase difference due to differences in the carrier frequency δf_n, $\delta\phi_n^{(s)}$ is the residual phase difference between the required and estimated beamsteering phase shift, and $\delta\phi_n^{(c)}$ is a constant phase due to system factors, including delays through the transceiver and the antenna phase pattern, among others. The residual beamforming phase error results from the imperfect estimation of the phase weights required to achieve a coherent wavefront in a given direction. The necessary phase at a given node n may be determined in reference to another node in the array or to a known global location, which need not be in the array. The beamsteering phase per node is $\phi_s = 2\pi(d_n/\lambda)\sin\theta_n$, where λ is the wavelength of the beamforming signal, d_n is the distance between the node and the reference point, and θ_n is defined relative to the baseline vector between node n and the reference point, which may be an adjacent node or location within the array [21]. Note that this pairwise approach provides a path toward extensibility to three dimensions. Thus,

the node must estimate its distance to the reference point and its beamsteering angle, yielding an estimated steering phase $\phi_e = 2\pi((d_n + \delta d_n)/\lambda)\sin(\theta_n + \delta\theta_n)$, where δd_n is the distance estimation error and $\delta\theta_n$ is the angle estimation error. The residual phase error is $\delta\phi_n^{(s)} = \phi_s - \phi_e$.

Based on the model above, there are a few principal factors that must be estimated and corrected to ensure the signals arrive at the destination coherently. These include the relative frequencies of the oscillators on each node, the distance between each node and a reference location, the relative timing offsets, the phase delays through each transceiver system, the phase errors resulting from imperfect oscillator synchronization, the beamsteering angles, and the channel delays from each node to the destination. Despite the inclusion of these errors, this model is nonetheless highly idealized compared to a physical implementation of a distributed array, and the list of secondary errors that may impact the coherence of a distributed beamforming operation is extensive, albeit increasingly application-dependent. An inexhaustive list includes angle-dependent antenna phase patterns manifesting on directional antennas; vibration-induced platform movement and oscillator drift on rotor aircraft; platform orientation changes causing antenna depolarization; Doppler-induced errors from relative platform motion; and geometric differences between antenna phase centers on those used for internode range estimation and those used for distributed beamforming. However, many such secondary errors may either be mitigated or may be negligible depending on the specific application. For instance, wide-beam antennas have fairly constant phase patterns in their mainbeam, platform vibration is minimal on satellites, depolarization can be overcome with circularly polarized antennas, formation flying yields negligible internode Doppler shifts, and antenna phase center mismatch can be mitigated by using the same antenna for both ranging and beamforming. However, regardless of the application and the secondary errors that may manifest, the principal errors described above must be addressed to support distributed beamforming to arbitrary angles.

The focus in this article is on coordination errors that can be addressed through microwave system design, specifically those errors that directly contribute to relative phase differences that will degrade beamforming, such as frequency synchronization and internode ranging. The impact of the channels (both node-to-destination and node-to-node) may be approached using channel estimation techniques [38]–[40] or may be negligible in specific but important cases, such as beamforming from aerial platforms to a far-field destination, as is the case of satellite or UAV swarms; in such cases, multipath between nodes will be minimal, and the node-to-destination channels can reasonably be assumed to be the same such that only beamsteering phase corrections due to node locations and beamsteering angles are necessary. Channel impacts are, thus, not considered in this work, which emphasizes the challenges that microwave technologies can address.

B. Coordination Requirements

The impact of the principal errors must be characterized to determine the level to which the errors must be estimated and mitigated. A metric that captures the impacts of errors in a very general way is the level of coherent gain achieved at the destination, defined as the signal power of a beamforming operation with the errors described above relative to that of an ideal beamforming operation. The coherent gain can, thus, be defined as

$$G_c = \frac{\left|s_r s_r^*\right|}{\left|s_i s_i^*\right|}. \tag{3}$$

The coherent gain varies between $0 \leq G_c \leq 1$, where $G_c = 1$ represents the highest achievable coherent gain. Representing the principal errors as random variables, the impact on the coherent gain of one or more error terms can be evaluated statistically. A useful approach is to determine the probability that a beamforming operation will obtain at least a specified level of coherent gain given the statistical parameters of one or more error terms, where common threshold values are $G_c \geq \{0.7, 0.8, 0.9\}$, representing, respectively, degradation in the beamforming gain of approximately 1.5, 1, and 0.5 dB. The probability that the coherent gain achieves this level, e.g., $P(G_c \geq 0.9)$, may then be evaluated statistically.

The requirements for estimating the principal errors are summarized here from [21] and [41]. Fig. 6 shows $P(G_c \geq 0.9)$ as a function of the standard deviations of the phase error $\delta\psi$ for various array sizes, with other errors set to zero. The results were obtained from 10 000 Monte Carlo simulations with normally distributed phase error and the steering angle taken as a uniform random variable over $[0, 2\pi)$. As the number of elements in the array increases, the threshold on the relative phase error between the oscillators at which the coherent gain is assured to be no less than 0.5 dB of the ideal level is approximately 18°. This error is inclusive of all phase errors, including system phase delays, oscillator phase differences, integrated phase walks due to frequency differences, and beamsteering errors. While oscillator and hardware phase errors can be addressed through wireless frequency synchronization or calibration, the beamforming phase errors are dependent on the locations of the nodes in the array, and thus, the tolerance on estimating the distance and angle in

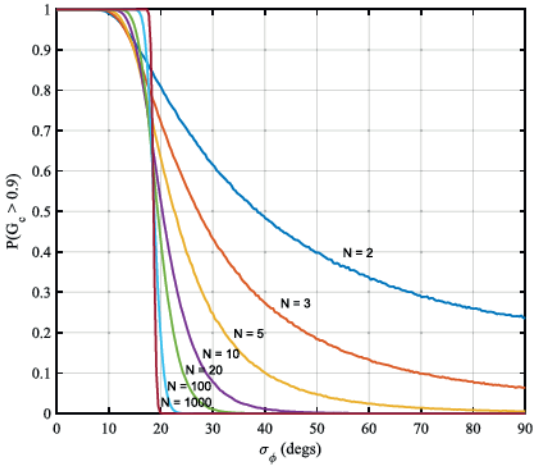

Fig. 6. Probability that the coherent gain will degrade by no less than 0.5 dB ($G_c \geq 0.9$) as a function of internode range estimation error. As the number of nodes increases, the requirement approaches 18°. From [21].

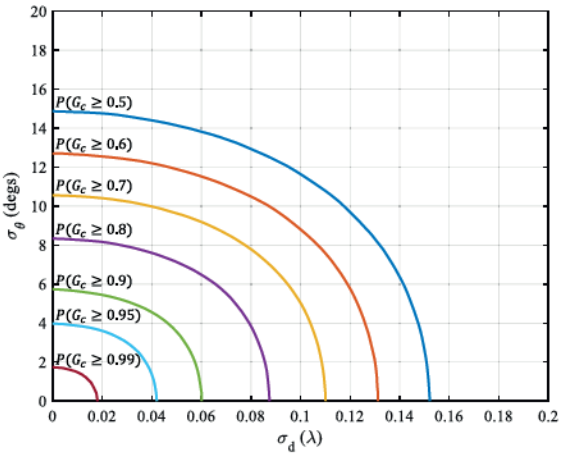

Fig. 7. 90% probability threshold $P(G_c \geq X)$ for various coherent gain values (legend) versus range estimation and normalized angle estimation error for $N = 10$. The angle estimation error is normalized by the wavelength. From [21].

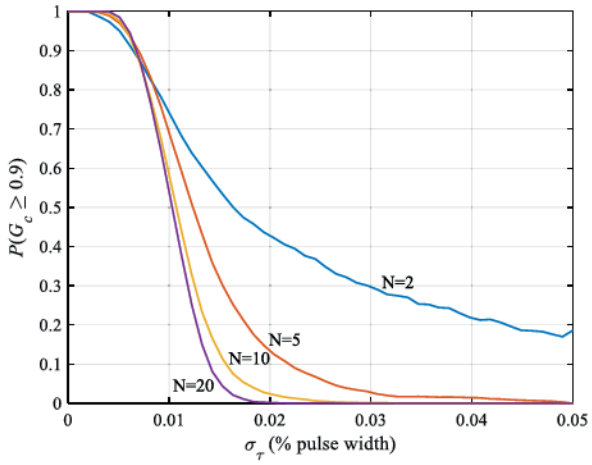

Fig. 8. Impact of timing errors for a 13-segment Barker coded waveform of duration T. From [41].

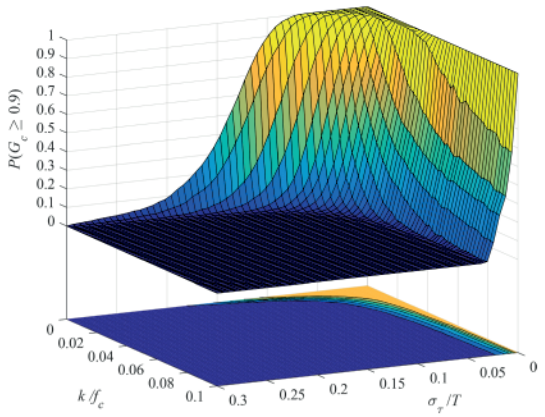

Fig. 9. Impact of timing errors for an LFM waveform of duration T and normalized modulation rate k/f_c for $N = 10$. From [41].

the beamsteering phase must be considered. The joint probability at various levels as a function of steering angle and ranging error is shown in Fig. 7, generated from 10 000 Monte Carlo simulations. If the beamforming angle is very accurate, internode range errors of no more than $\lambda/15$ can be tolerated; this error is, however, compounded when phase errors due to wireless frequency transfer are considered or when steering toward endfire [21], [42].

Angle estimation errors also contribute to the degradation in coherent gain, as shown in Fig. 7, which shows the joint probability of the coherent gain as a function of normally distributed range and angle errors. The angle error is normalized by wavelength; for an internode distance d wavelengths, the angle standard deviation is σ_θ/d. For example, to achieve $G_c \geq 0.8$ with high probability with a ranging standard deviation of 0.07λ, the normalized angle standard deviation is 6°; for a 10-m internode distance and a 1-GHz carrier frequency, angle estimation of approximately 0.2° standard deviation is necessary. While some techniques can theoretically achieve accuracies below this value (e.g., [43]–[45]), practical implementations are challenging.

The previous errors impact the ability to maintain a steered monochromatic signal; however, signals carrying information must also be appropriately aligned in time such that their envelopes appreciably overlap at the destination. Generally, this timing requirement is inversely dependent on the bandwidth and the modulation of the waveform. For a simple amplitude-modulated pulse on a single carrier frequency, it is apparent that a waveform overlap of 90% will ensure $G_c \geq 0.9$; however, the requirements are more stringent for waveforms with phase or frequency modulation [41]. Figs. 8 and 9 show $P(G_c \geq 0.9)$ for a Barker-coded radar waveform and a linear-frequency modulated (LFM) pulse.

IV. Subsystem Synchronization Technologies

This section discusses recent developments in microwave and millimeter-wave systems for high-accuracy localization, wireless frequency transfer, and time alignment, to address the three principal coordination challenges discussed above.

A. Internode Range Estimation

Distributed beamforming necessitates accurate localization of the nodes in the array, especially for open-loop systems that do not rely on external feedback to support phase-coherent beamforming to desired directions. Accurate internode ranging represents the basis for accurate node localization and, consequently, sufficient phase alignment. As noted above, a range estimation root-mean-square error (RMSE) of $\lambda/15$ is needed to have a 90% probability to achieve 0.9 coherent gain considering the range estimation error in isolation (no other errors). In [42], the effect of wireless frequency synchronization in a centralized topology was considered, where the frequency synchronization signal undergoes a phase shift due to propagation between the nodes, and the requirement for the ranging RMSE was shown to be more stringent, $\lambda/26$. Thus, for microwave frequencies and above, the required range estimation RMSE is on the order of centimeters or millimeters. In dynamic systems, this level of accuracy needs to be achieved quickly, before the nodes move out of the coherence length.

High-accuracy ranging at the sub-cm level is feasible using optical systems due to their large instantaneous bandwidth; however, optical links require accurate pointing and tracking hardware on every node, including gimbals and adaptive

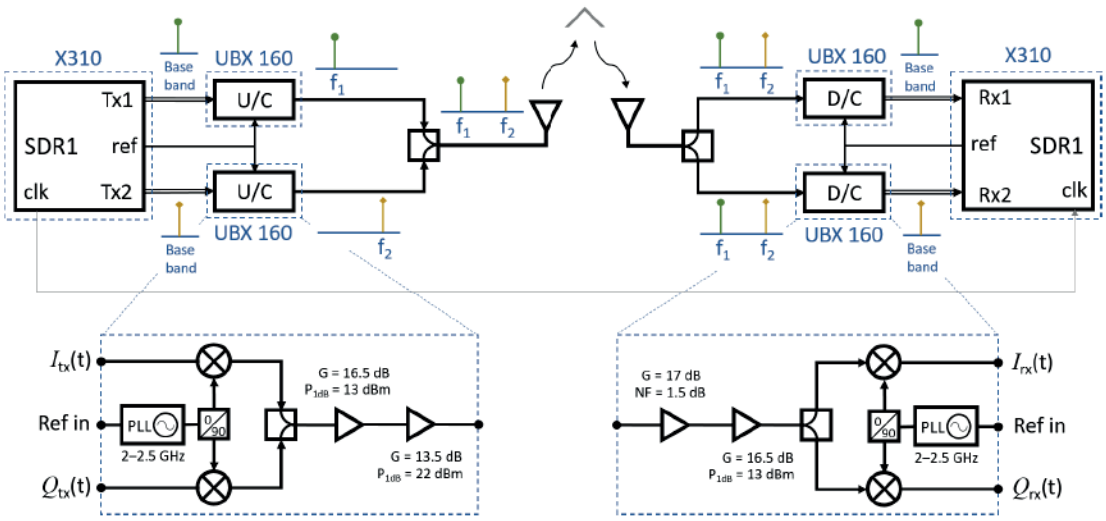

Fig. 10. Block diagram of the spectrally sparse ranging system. Each tone was generated by a separate daughterboard; afterward, the two signals were combined and transmitted. The received signal is split fed to the receive inputs. The resulting baseband signals are digitally reconstructed to their tone separation in the air. U/C = upconverter, D/C = downconverter, PLL = phase-locked loop, G = gain, and NF = noise figure. From [46].

optics, and are thus not scalable to large arrays [47], [48]. Ranging waveforms have been extensively studied in [49], [50], through which it was shown that two-tone signals have the lowest Cramer–Rao lower bound (CRLB) on delay estimation. The CRLB gives the minimum achievable variance in time delay estimation, given by [51]

$$\sigma^2 \geq \frac{1}{\beta^2 \frac{2E}{N_0}} \tag{4}$$

where E is the signal energy, N_0 is the noise power spectral density, and β^2 is the mean-square bandwidth, or the effective bandwidth of the signal, where

$$\beta^2 = \frac{\int_{-\infty}^{\infty} (2\pi f)^2 |S(f)|^2 df}{\int_{-\infty}^{\infty} |S(f)|^2 df} \tag{5}$$

with $S(f)$ denoting the Fourier transform of the temporal signal for a given frequency f. It can be seen that β^2 is the normalized second moment of the signal spectrum. This implies that accurate range estimation is obtained not just by increasing the signal bandwidth, but by concentrating the signal energy into two narrow sidebands. This dual-tone waveform was tested in [52], where, for 500-MHz tone separation and 27.5-dB SNR, the ranging standard deviation was 0.2 mm. It is important to note that high SNR values can be achieved between nodes in a distributed phased array due to the cooperative nature of the system: a repeater can be added to the nodes to boost the signal with gain, overcoming the R^{-4} losses.

The benefits of the two-tone waveform extend to the hardware domain as well. While it is challenging to develop hardware that reliably supports very wide bandwidth signals, a two-tone waveform can be directly generated and received using two separate, phase-locked transceivers. The received signals, individually narrowband, can be sampled with low-rate digitizers and digitally reconstructed to their wideband tone separation for accurate matched filter processing. This approach was demonstrated using a dual-channel

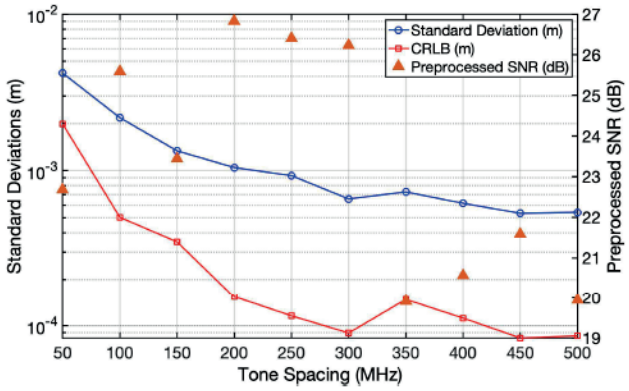

Fig. 11. Measured wireless range estimation accuracy. At a tone spacing of 450 MHz, the ranging accuracy was 530 μm. From [46].

microwave sensor in [46], where each tone was generated and received by a separate transceiver. The block diagram of the ranging system is shown in Fig. 10, and the results are shown in Fig. 11, where the ranging accuracy of 530 μm was obtained with a 450-MHz tone separation on the two narrowband transceivers.

The CRLB of multitone signals was studied in [53] where it was shown that adding additional tones or bandwidth to one or both of the dual-tone signals has a minimal impact on the lower bound. Such multitone signals can be used for joint ranging and frequency transfer in centralized systems. Nevertheless, two-tone or multitone signals are ambiguous in nature, and their application can be limited to a small number of nodes. This issue was resolved in [54] where two-tone stepped-frequency waveforms (TTSFWs) were developed to combine accuracy and scalability.

Although two-tone signals have the highest accuracy, one can select any waveform for ranging. In the cases where ranging accuracy is not the only concern, different waveforms could be more desirable. As an example, frequency-modulated continuous-wave (FMCW) radar systems [55]–[60] are of interest for a wide variety of distributed systems due to their

good accuracy and small range resolution (on the order of centimeters or sometimes millimeters). In [59], an accuracy of $\approx$ 1 mm was reported for a 2-GHz ranging bandwidth. A 75-GHz FMCW radar with 2-GHz bandwidth, 2-ms sweep time, and averaging of 2000 samples was used in [60]. The system was able to achieve a ranging standard deviation of 0.1 mm and a standard deviation in angle direction of 0.05°. Other works implemented FMCW radars with much higher bandwidth and achieved even higher accuracies. For example, in [61], a 25.6-GHz bandwidth was used with a carrier of 80 GHz, and a ranging standard deviation of 4 μm was achieved for close targets.

B. Frequency Synchronization

Frequency synchronization is essential for coherent distributed arrays and any radio frequency (RF) cooperative application in general. Since the transmitters in a distributed array are physically separated, frequency synchronization needs to be performed wirelessly. In orthogonal frequency-division multiple access (OFDMA), wireless frequency synchronization ensures the suppression of multiple access and interchannel interferences, and it allows proper orthogonality. In OFDMA, usually, time is synchronized first, and then the frequency is aligned [62]. In distributed phased arrays, typically, the first electrical state that needs to be synchronized is the frequency. Without frequency synchronization, phase alignment is not possible, and clocks on the distributed nodes will drift continuously. Various techniques have been developed for wireless frequency synchronization, many of which fall in the closed-loop or retrodirective category, where feedback from the target or receiver is needed [23], [63], [64]. A receiver-coordinated time-slotted approach was used in [23] to allow the receiver to estimate each of the transmitters' phase separately. Afterward, the feedback at every transmitter was fed to a Kalman filter to predict the phase and frequency shifts. Other closed-loop methods, such as in [63], perform the necessary frequency and phase adjustments depending on the received power at the targeted location, where the phase and frequency are modified until maximum power is received. In [64], the nodes transmitted signals with a predetermined reference frequency to the receiver, which then used these signals to estimate the carrier frequency offset at each node. Although promising results are obtained for closed-loop architectures, their application is limited to the scenarios where the transmitters and the destination are able to coordinate.

Other wireless frequency synchronization techniques include synchronization using coupled-oscillators [65]. The main drawback of these techniques is that it is affected by the separation distance of the nodes. Optically locked voltage-controlled oscillators were studied in [66]; however, optical links are not always a viable option, especially in widely separated connections, where pointing, tracking, and acquisition require special hardware on each node. In many applications, GPS signals were used for wireless frequency synchronization [67], but, as mentioned earlier, GNSS signals are not always available, and an alternative method is desirable for many applications.

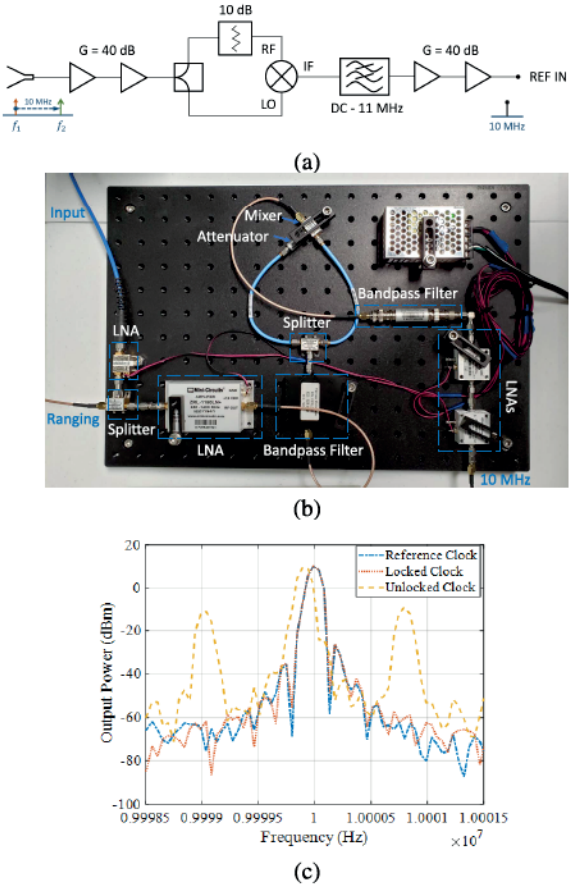

Fig. 12. (a) Self-mixing frequency locking circuit block diagram. (b) Circuit used by the secondary nodes, which outputs the ranging returns and the 10-MHz reference signal that is fed to the PLL internal to the secondary SDRs. (c) Measured frequency output compared to the reference signal when locked and unlocked. From [72] and [73].

Centralized approaches where secondary nodes synchronize to a primary node have been extensively studied in the literature. In centralized approaches, many works focused on taking advantage of the phase-locked loops (PLLs) internal to software-defined radios (SDRs) or other hardware available on the nodes. In [68], a signal was transmitted from a primary node to lock the frequency of the secondary nodes using their internal PLLs. However, this approach lacks flexibility as the frequency of the transmitted signal must be exactly equal to the required input frequency of the PLLs. In [69] two cascaded PLLs were implemented to resolve this issue, where the received signals go through an intermediate PLL that scales the frequency using multipliers and dividers. Yet, transmitting only a single frequency is prone to interference. Spectrally sparse signals were used in [70] and [71] to overcome this problem. The signal was formed by two tones with a tone separation equal to the desired input frequency for the PLLs. A self-mixing circuit was used at every secondary node to demodulate the desired signal. The design of the reference frequency transmitter and the self-mixing circuit is shown in Fig. 12, along with an implementation and measured frequency output.

The main drawback in centralized topologies is that, in widely separated arrays, one node transmitting the reference

signal might not be enough. Decentralized frequency synchronization was developed in [74] to increase the flexibility in an array and prevent any problems in the case of a primary node failure. In this approach, the nodes were adjusting their carrier frequency to reach a final average frequency among all the nodes. Phase tracking in such approaches might be more complicated than the previous ones since the frequency on every node is constantly changing to follow a general frequency consensus.

C. Time Alignment

In general, distributed phased arrays require appropriate time alignment so that the transmitted pulses or symbols overlap sufficiently. Transmissions from distributed arrays need to be aligned to a fraction of the signal bandwidth, making the requirements for time alignment much more tolerant than the requirements for phase alignment. Nevertheless, for wideband signals with hundreds of MHz of bandwidth, timing errors on the order of nanoseconds or sometimes picoseconds are required [75].

Generally, the internal clocks at each node are disciplined by at least one oscillator that drifts over time. As a result, a simplified model describing the relative clocks at two nodes can be given as [76]

$$C_1(t) = a \cdot C_2(t) + b \tag{6}$$

where a is the relative drift and b is the relative offset between the clocks 1 and 2. For perfectly synchronized clocks, one must have $a = 1$ and $b = 0$. Time alignment is generally feasible using common time transfer systems, such as GPS and network time protocol (NTP). Nevertheless, GNSS signals are not always detectable, especially indoors, and the accuracy achieved using GNSS and NTP systems is not generally adequate for beamforming applications at most frequencies of interest. Furthermore, these systems increase energy consumption, hardware complexity, and cost. To overcome these issues, multiple clock synchronization methods for networked wireless systems have been developed in the literature. Initially, most of the time alignment methods focused on transmitting the timestamps from one node to the other to synchronize the clocks. Recently, time alignment techniques have shifted toward timestamp-free approaches that offer added accuracy, simplicity, and flexibility.

The Timing-Sync Protocol for Sensor Networks (TPSN) [77] is one of the most notable time transfer techniques that use timestamps to achieve time alignment in a distributed array. TPSN synchronizes networks in a two-phase framework, including a level discovery phase and a synchronization phase. In the level discovery phase, the nodes are assigned levels from 0 to n, where the nodes with level n synchronize to nodes with level $n-1$. This phase starts by assigning level 0 to a node, which is usually synchronized to an external device. The level 0 node broadcasts a discovery signal to the surrounding nodes, which, in turn, label themselves with level 1. Afterward, level 1 nodes broadcast the discovery signals to find the level 2 nodes, and so on. After discovering the entire array,

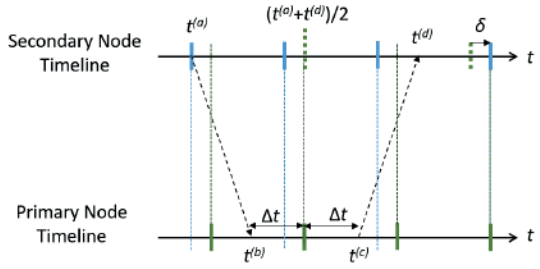

Fig. 13. Timestamp-free synchronization protocol (adapted from [79]).

the synchronization phase happens between a pair of nodes from two consecutive levels, starting with levels 0 and 1. The synchronization is done by transmitting from node 1 to node 0 at time t_1, a synchronization pulse containing the level of node 1 and the time t_1, and node 0 receives the pulse at $t_2 = t_1 + \delta + d$, according to its clock, and retransmits a signal at t_3 containing the level of node 0, and the values t_1, t_2, and t_3. δ refers to the relative clock drift between the nodes, and d refers to the propagation delay between the nodes. Once the pulse is received at t_4, the node synchronizes itself to node 0 by estimating the clock drift and the propagation delay using

$$\delta = \frac{(t_2 - t_1) - (t_4 - t_3)}{2}, \tag{7}$$

$$d = \frac{(t_2 - t_1) + (t_4 - t_3)}{2}. \tag{8}$$

In this process, the drift and the propagation delays are assumed constant throughout the synchronization process.

Tiny-Sync (TS) and Mini-Sync (MS) [78] are other time synchronization approaches that rely on timestamps and the model in (6). In both approaches, node 0 transmits a synchronization pulse with a timestamp t_1 generated right before the transmission. Node 1 generates a timestamp t_2 when it gets the message and sends it back. Once node 0 receives the message at t_3, it generates a timestamp. Using the timestamps and (6), the following equations are obtained:

$$t_1 < a \cdot t_2 + b, \tag{9}$$

$$t_3 > a \cdot t_2 + b. \tag{10}$$

Multiple synchronization pulses are transmitted to have a large set of inequalities describing the coefficients a and b. Both TS and MS work on finding the optimal a and b out of the inequalities, where MS is an extension of TS that is designed to keep the data points that can be useful for future time synchronizations.

All the mentioned time alignment approaches so far rely on exchanging timestamp information or other timing data at the MAC layer. Using the medium access control (MAC) layer increases the complexity and delays, and prevents the system from having accurate time alignment, as all these approaches have timing errors on the order of microseconds [76]. To overcome this issue, a timestamp-free approach was developed in [79]–[81], where the functionality was moved to the physical layer (PHY). Doing so increases the accuracy of time alignment dramatically and allows fast synchronization.

In this protocol, as described in Fig. 13, the secondary node n transmits a packet or pulse to the primary node at a local time $t^{(a)}$. The primary node receives the packet at its local time $t^{(b)}$ and retransmits a packet back to the secondary node at time $t^{(c)}$, where $t^{(b)}$ and $t^{(c)}$ are symmetric around the primary clock tick such that $((t^{(b)} + t^{(c)})/2) (\text{mod } T_0) = 0$, where T_0 is the clock tick period of the primary node. This way, the clock tick of the primary node will be located between $t^{(b)}$ and $t^{(c)}$. Due to channel reciprocity, the secondary node receives the packet back at $t^{(d)}$. By doing so, the secondary node is able to estimate its clock tick offset with respect to the primary node using

$$\delta = \left(\frac{t^{(a)} + t^{(d)}}{2} \right)_{T_0} \tag{11}$$

where the notation $(x)_{T_0}$ refers to wrapping x to the interval $[-T_0/2, T_0/2)$. A wireless time alignment approach based on this concept was demonstrated in [75] on NI 2943R USRPs. In this work, the synchronization pulse was a 1-μs, 40-MHz LFM signal at 1.44 GHz. A standard deviation of less than 100 *ps* was observed in the testing.

V. Experimental Demonstrations

The coordination technologies described above enable distributed beamforming in various forms. This section describes examples from the recent literature of closed- and open-loop distributed beamforming experiments.

A. Receive Beamforming With Frequency Synchronization

Distributed phased arrays performing only receive beamforming can be implemented with less coordination than arrays performing transmit beamforming. This section presents an experimental example of a distributed receive beamforming architecture based only on frequency synchronization conducted by the authors in 2020. The array consisted of a set of receivers with locked local oscillators receiving a pulsed emission from a separate node (see Fig. 5). The set of received signals $\mathbf{s}_{rx} = \{s_{rx}^{(1)}, s_{rx}^{(2)}, \ldots, s_{rx}^{(N)}\}$ was collected and coprocessed. The phase of each received signal was estimated by calculating the phase of the Fourier transform of the received signals, $\phi_n = \angle \mathcal{F}\{s_{rx}^{(n)}\}$. The signals were then phase-shifted and summed yielding the beamformed signal $s_{rx}^{bf} = \mathbf{s}_{rx}\Phi^*$, where $\Phi^\intercal = \{e^{j\phi_1}, e^{j\phi_2}, \ldots, e^{j\phi_N}\}$. This approach was tested on a set of four Ettus X310 SDRs. One radio transmitted a pulsed waveform that was captured by a three-node receiving array, as shown in Fig. 14(a) and (b), which shows the diagram of the setup and the system in the lab. The waveform was a pulsed continuous-wave (CW) signal at 5 GHz with a pulsewidth of 2 ms. The local oscillators of the three receiving antennas were locked via cable. Fig. 14(c) (top) shows the real part of a section of the time-domain waveforms captured on each of the three nodes without phase correction (in blue thin lines) and the real part of the summed signals (the black thick line), demonstrating that summation of the signals without phase correction leads to a degradation in the overall signal amplitude. Fig. 14(c) (bottom) shows the same signals over the same time span after estimating and correcting the signal phases. It is clear that the individual waveforms align closely in phase, and the beamformed signal (the black thick line) demonstrates a significant increase in signal amplitude compared to the signals without phase correction. While this approach demonstrates the ability to align the carrier frequencies, time alignment must also be implemented in cases where the relative propagation delay between the receiving nodes is a large fraction of the information length carried on the signal. Furthermore, fast signal modulation or signal interference may complicate the ability to accurately estimate the signal phase.

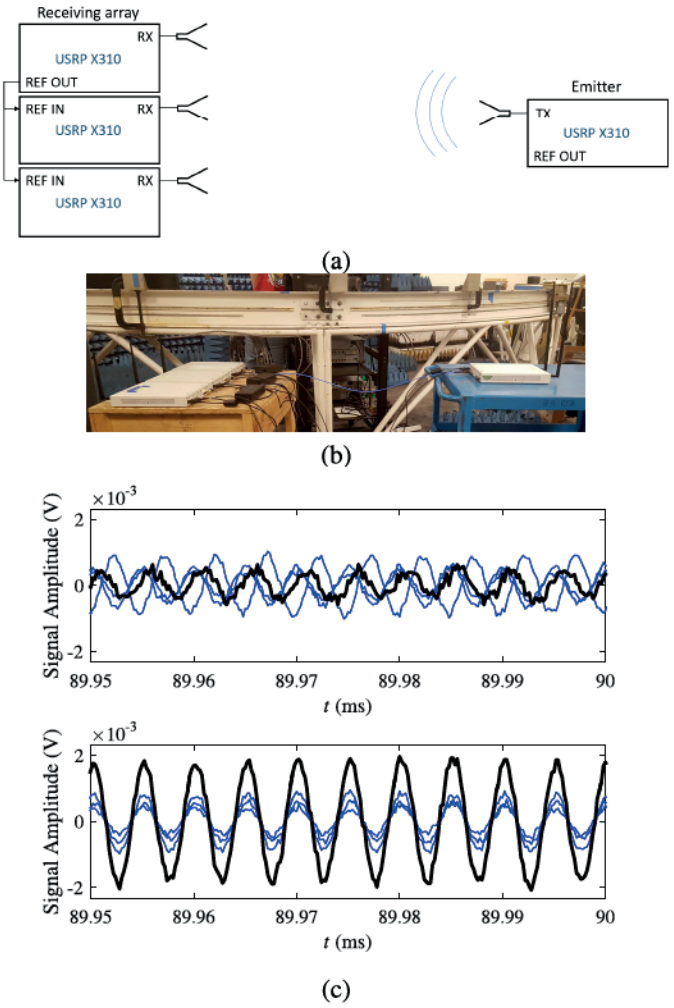

Fig. 14. (a) Diagram of a distributed receive beamforming system. (b) Experimental setup of the three-node distributed receive beamforming system consisting of four Ettus X310 SDRs. The distributed receive array consisted of three radios, with the fourth radio used as a transmitter. The three radios were only coordinated by synchronizing their internal oscillators. (c) Received signals at each of the three receivers (in blue) and the beamformed signal obtained by superposition of the three signals (in black). Top: unoptimized received signals and resulting beamformed signal, clearly showing a reduction in overall signal amplitude due to phase errors. Bottom: optimized beamformed signal showing a clear alignment of the individual signals and an increase in the amplitude of the beamformed signal.

B. Feedback-Enabled Closed-Loop Systems

Implementing coherent distributed arrays, in general, is challenging; however, closed-loop architectures are easier to implement since fewer electrical states need to be coordinated

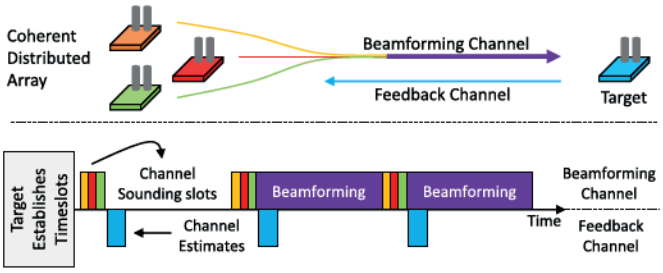

Fig. 15. Receiver coordinated distributed beamforming architecture (adapted from [23]). Each transmitter transmits its uncompensated carrier using an assigned time slot. Based on these transmissions, the target sends feedback containing the channel estimates. These estimates are used to align the phase and frequency of the nodes to allow coherent beamforming.

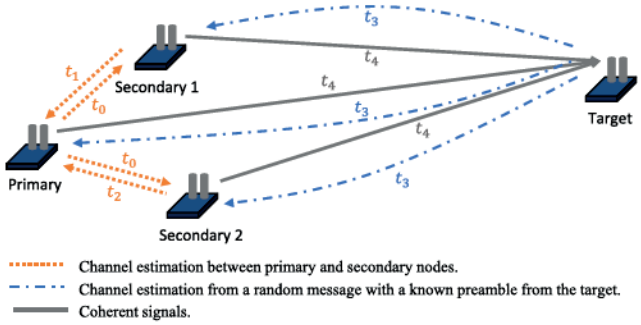

Fig. 16. Retrodirective beamforming approach used in [27]. Synchronization is based on assigning time slots to synchronize the frequencies of the secondary nodes to the primary node, estimate the channels between the nodes and the target, and beamform to the target.

directly between the nodes in the array. An example of distributed transmit beamforming includes [82], where frequency and phase synchronization was accomplished through feedback from the receiver. In this work, the transmitters were each receiving a feedback packet from the receiver containing information to adjust their phase and frequency independently of each other. Frequency locking and beamsteering were decoupled although both of them used the same packet for synchronization. An extended Kalman filter tracked the phase and frequency offsets of the modulated waveforms in the feedback packet in order to lock the receiver frequency, while the transmitted phase was modified based on 1-bit feedback containing the change in received signal strength [24]. The phase synchronization worked as follows: at each time slot, the transmitters added $+15°$ or $-15°$ perturbation to their current phase, and a correction was made depending on the increase or decrease in the received signal strength feedback. Phase errors below 15° were obtained with feedback rates above 15 Hz, yielding beamforming gain close to the ideal level.

Another type of closed-loop beamforming was shown in [23], where the carrier phases of the transmitters were measured by the receiver using a time-slotted approach and then fed to Kalman filters at the transmitting nodes to detect the offset in phase and frequency. The beamforming approach is illustrated in Fig. 15. First, the receiver determines the time slots, and then, each transmitter is assigned a sounding period in between the beamforming slots. In the sounding period, the transmitters send their uncompensated carrier, and the receiver determines the carrier phase offset. The offsets are sent back as feedback, and the Kalman filters are used to predict the phase and frequency offset at the start of the beamforming slot. Finally, a phase and a frequency offset are applied before the beamforming slot. Experimental results were taken at 910 MHz using CW signals. The transmitters were 1 km away from the receiver and were sequentially activated, demonstrating a gradual increase in beamforming gain, until obtaining a beamforming gain within 0.1 dB of ideal with all transmitters.

C. Retrodirective Distributed Arrays

Retrodirective coherent distributed arrays are more challenging to implement than cooperative closed-loop systems since less information can be received from the target. In [27], retrodirective beamforming was achieved for a hierarchical system with stationary nodes, where the transmitting nodes and the target were each assigned a time slot to exchange messages. As shown in Fig. 16, the first time slot was assigned to the primary node and then subsequently each secondary node with the target in the final time slot. This message exchange order, which is repeated every epoch, is used to determine the frequency offset of the secondary nodes in comparison to the primary node and estimate the effective complex channel gains between the primary and secondary nodes, and the effective complex channel gains between the target and the other nodes. In the first time slot, the secondary nodes estimate their individual frequency offsets and channel gains relative to the primary node. Each secondary node then transmits in sequence back to the primary node, which determines the channel gains. The target node then sends an arbitrary message with a known preamble to all the nodes, which is used to determine the effective channel gain from each node to the target. Following this, in the last time slot, the array transmits coherently to the target. Experimental results with one primary node and two secondary nodes were presented in [27], where phase errors less than 1° were observed, well below the 18° threshold, and the array obtained beamforming gain at the target node of greater than 90% of the ideal beamforming gain after a convergence period of about 10 s. Once converged, the system was relatively stable. It should be noted that most distributed beamforming approaches require some form of initial calibration or convergence to a coherent state, and a delay of a few seconds could impact system performance in dynamic environments. Improving system factors, such as the speed of frequency synchronization and the channel estimation, could reduce the convergence time.

D. Open-Loop Systems

Open-loop distributed beamforming is the most challenging topology to implement; however, recent research has begun to demonstrate open-loop beamforming based on the coordination technologies described above. In open-loop architectures, phase alignment is performed by monitoring the relative positions of the nodes to determine the relative phase shift. This can be accomplished with a centralized system where secondary nodes localize themselves in reference to

a primary node and, based on their relative position, update their transmitted signal phase. This method alleviates the need to have connections between all the nodes in an array and, consequently, mitigates the burden of using time division for data transfer, which is not suitable for large arrays. While beamforming to the far-field, the phase delay due to platform motion is the only dynamic phase parameter that must be estimated during beamforming. An initial calibration of the static phase delays in the hardware of each node is necessary; however, this generally only needs to be completed once since the phases are static. In [54], high-accuracy internode ranging in a centralized coherent distributed array was demonstrated. The TTSFW was used for ranging; this ranging waveform combines the high accuracy of two-tone waveforms and the scalability of stepped frequency waveforms and alleviates the ambiguous nature of dual-tone waveforms by effectively creating a discrete wideband signal. The TTSFW was modeled as

$$S(t) = \frac{1}{\sqrt{N}} \sum_{n=0}^{N-1} \text{rect}\left(\frac{t - nT_r}{T}\right)\left(e^{j2\pi f_1 t} + e^{j2\pi f_2 t}\right)e^{j2\pi n\delta f t} \tag{12}$$

where N is the number of encoding pulses, T is the pulse duration, T_r is the nonzero duration of each pulse, f_1 is the starting frequency with a monotonic increase by δf increments, the step frequency $\delta f = (\text{BW}/2N - 1)$, BW is the available bandwidth, and $f_2 = f_1 + N\delta f$. Every secondary node used the same ranging waveform but with a different encoding. The primary node was equipped with an active repeater that amplifies the received signals and retransmits them back to their source using another carrier. The use of an active repeater improved the ranging performance as the received ranging pulses had a much higher SNR in comparison to the cases where no repeater was used. Also, the repeater allowed the primary node to be perceived as a point source, which is necessary for accurate range estimation. The experimental setup and results are shown in Fig. 17. The plot shows the signal levels of individual transmitters, the ideal combined signal level, beamforming signal level without correcting the dynamic phase changes due to motion, and beamforming signal level with the ranging system correcting the dynamic phase changes. The following values were selected in this experiment: $N = 4$ and $\delta f = 1$ MHz. Range estimation accuracy in this work was sufficient to support beamforming up to 9.4 GHz based on the $\lambda/15$ metric. Additional details on these experimental results are available in [54]. Using this system, the authors conducted the beamforming experiment using SDRs at a 1.5-GHz carrier frequency. As shown in Fig. 17(b), when the phase changes are not corrected, the beamforming signal level undergoes destructive interference, yielding a null (near the middle of the plot). When the ranging system measured the motion and the phase was corrected in response to this measurement, the beamforming gain obtained nearly ideal signal levels, above the 90% threshold throughout the measurement.

In [83], a two-tone ranging waveform with 200 MHz tone separation along with a disambiguation pulse was used to monitor the internode range. Once a change in internode

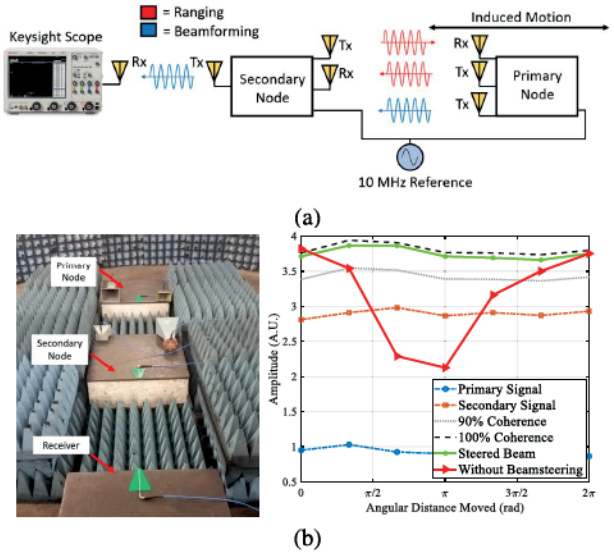

Fig. 17. (a) Schematic of an open-loop distributed beamforming system using the cooperative ranging technique. (b) Image of the experimental setup and measured results showing beamforming using the phase correction from the ranging system as the nodes move, and the uncorrected received signal. Additional details are available in [54].

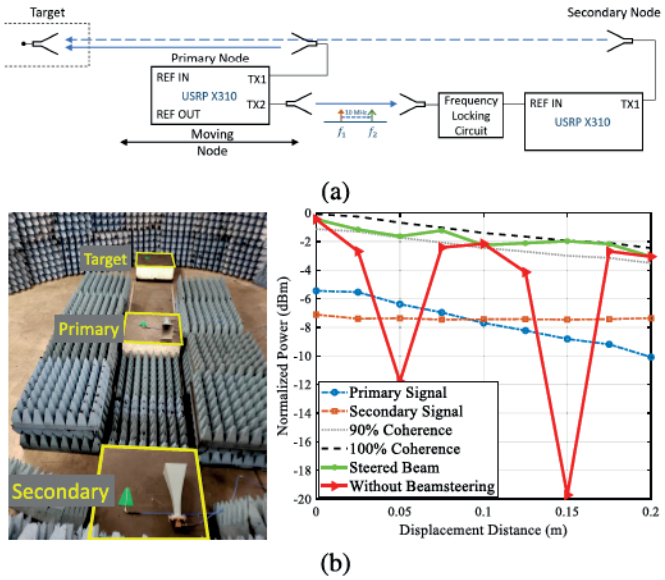

Fig. 18. (a) Diagram of an open-loop distributed beamforming system using wireless frequency transfer. (b) Image of the experimental setup and coherent beamforming results showing the combined signal power of the two transmitted signals for multiple displacement distances of the primary node. From [71].

separation was detected, the phase of the secondary node was adjusted to achieve coherent beamforming. Testing was done outdoors over a beamforming distance of 520 m. In this test, the frequencies of both nodes were locked to a 10-MHz reference via cable connection, and one node was moved; thus, the ranging system estimated the appropriate phase correction required for beamsteering only from the change in internode distance and updated its transmit signal accordingly, demonstrating the ability to maintain a steered beam in an open-loop architecture.

In [71], open-loop distributed beamforming was achieved using a hierarchical two-node system based on wireless

frequency transfer. A self-mixing circuit was used by the secondary node to recover a reference frequency transmitted by the primary node via a two-tone signal with a 10-MHz tone separation. The recovered 10-MHz signal was fed to the PLL of the secondary node to lock the oscillators. The phase shift introduced from the wireless frequency synchronization circuit for nodes in relative motion is

$$\Delta\phi_{c,1} = -2\pi \frac{\Delta d_{IN}}{\lambda_c} \tag{13}$$

where Δd_{IN} is the displacement distance separating the frequency synchronization antennas and λ_c is the beamforming wavelength. Once $\Delta\phi_{c,1}$ was determined, beamsteering was possible after accounting for the extra phase shift produced from the new distance of the secondary nodes, which can be found from

$$\Delta\phi_{c,2} = -2\pi \frac{\Delta d_T \cdot \sin(\theta)}{\lambda_c} \tag{14}$$

where Δd_T is the displacement distance separating the two transmitters, and θ is the beamsteering angle. Beamforming was achieved at 1.5 GHz, where the experimental setup and results are shown in Fig. 18. The plot shows the signal levels of individual transmitters, the ideal combined signal level, the beamforming signal level without correcting the dynamic phase changes due to motion, and the beamforming signal level with the ranging system correcting the dynamic phase changes. When the phase changes are not corrected, the beamforming signal level undergoes two points of destructive interference due to the effect of both platform motion and the phase delay of the wireless frequency signal. When the phase is corrected, the beamforming gain reaches nearly ideal signal levels. Additional details on these experimental results are available in [71]. Note that, in the above works, the transmitted signal was CW, which, in nature, does not require time alignment. In case time alignment is needed, one of the previously mentioned time alignment techniques can be implemented.

VI. Conclusion and Future Challenges

Implementation of a distributed phased array on practical platforms undergoing real-world dynamics is a difficult problem entailing a number of challenges in addition to those outlined in this article. Herein, the principal coordination challenges—phase alignment, frequency synchronization, and time alignment—were reviewed, microwave system solutions to these challenges were described, and experimental implementations based on these basic coordination technologies have been discussed. These experimental results demonstrate the feasibility of addressing the principal coordination challenges in distributed phased arrays.

A number of secondary challenges remain, which may be more or less important depending on the application. The requirements on the estimation of the internode angle, necessary for beamsteering, are quite stringent, more so at longer ranges. While theoretical angle estimation techniques indicate support for angle estimation errors to a fraction of a degree, practical implementations obtaining this level of estimation error are difficult to achieve. Channel estimation, both node-to-destination and node-to-node (internode), is likely necessary for wide node separations and high-frequency operation. Additional environmental concerns, such as multipath, non-line-of-sight connections, and signal interference on the coordination systems, can further impact the performance. Platform dynamics impart a number of positional uncertainties, including vibrations, rotations, and so on, which may impact internode range estimation and can affect the polarization of the transmitted signals. Phase patterns of the antennas implementing the beamforming operation impart a further phase error, particularly in high-gain antennas. This list is not exhaustive, and it is likely that additional challenges will be present.

Despite these remaining challenges, it is significant that the most basic coordination challenges have viable solutions for both closed- and open-loop distributed phased arrays. The technologies and demonstrations described in this article, thus, provide a framework for future distributed phased array research.

Acknowledgment

The views, opinions, and/or findings contained in this article are those of the authors and should not be interpreted as representing the official views or policies, either expressed or implied, of the Defense Advanced Research Projects Agency or the Department of Defense.

References

[1] I. F. Akyildiz, W. Su, Y. Sankarasubramaniam, and E. Cayirci, "Wireless sensor networks: A survey," *Comput. Netw.*, vol. 38, no. 4, pp. 393–422, 2002.

[2] W. Dargie and C. Poellabauer, *Fundamentals of Wireless Sensor Networks: Theory and Practice*. Hoboken, NJ, USA: Wiley, Nov. 2010.

[3] A. Frischen, J. Hasch, and C. Waldschmidt, "Contour recognition with a cooperative distributed radar sensor network," in *IEEE MTT-S Int. Microw. Symp. Dig.*, Apr. 2015, pp. 1–4.

[4] S. Schieler *et al.*, "OFDM waveform for distributed radar sensing in automotive scenarios," *Int. J. Microw. Wireless Technol.*, vol. 12, no. 8, pp. 716–722, Jul. 2020.

[5] E. Fishler, A. Haimovich, R. Blum, D. Chizhik, L. Cimini, and R. Valenzuela, "MIMO radar: An idea whose time has come," in *Proc. IEEE Radar Conf.*, Apr. 2004, pp. 71–78.

[6] S. Gogineni and A. Nehorai, "Target estimation using sparse modeling for distributed MIMO radar," *IEEE Trans. Signal Process.*, vol. 59, no. 11, pp. 5315–5325, Nov. 2011.

[7] D. Parker and D. C. Zimmermann, "Phased arrays—Part 1: Theory and architectures," *IEEE Trans. Microw. Theory Techn.*, vol. 50, no. 3, pp. 678–687, Mar. 2002.

[8] D. Parker and D. C. Zimmermann, "Phased arrays—Part II: Implementations, applications, and future trends," *IEEE Trans. Microw. Theory Techn.*, vol. 50, no. 3, pp. 688–698, Mar. 2002.

[9] C. Fulton, M. Yeary, D. Thompson, J. Lake, and A. Mitchell, "Digital phased arrays: Challenges and opportunities," *Proc. IEEE*, vol. 104, no. 3, pp. 487–503, Mar. 2016.

[10] S. H. Talisa, K. W. O'Haver, T. M. Comberiate, M. D. Sharp, and O. F. Somerlock, "Benefits of digital phased array radars," *Proc. IEEE*, vol. 104, no. 3, pp. 530–543, Mar. 2016.

[11] R. Mudumbai, G. Barriac, and U. Madhow, "On the feasibility of distributed beamforming in wireless networks," *IEEE Trans. Wireless Commun.*, vol. 6, no. 5, pp. 1754–1763, May 2007.

[12] Z. Ding, W. Chin, and K. Leung, "Distributed beamforming and power allocation for cooperative networks," *IEEE Trans. Wireless Commun.*, vol. 7, no. 5, pp. 1817–1822, May 2008.

[13] B. L. Ng, J. S. Evans, S. V. Hanly, and D. Aktas, "Distributed downlink beamforming with cooperative base stations," *IEEE Trans. Inf. Theory*, vol. 54, no. 12, pp. 5491–5499, Dec. 2008.

[14] V. Havary-Nassab, S. Shahbazpanahi, and A. Grami, "Optimal distributed beamforming for two-way relay networks," *IEEE Trans. Signal Process.*, vol. 58, no. 3, pp. 1238–1250, Mar. 2010.

[15] R. C. Hansen, *Phased Array Antennas*, vol. 213. Hoboken, NJ, USA: Wiley, Nov. 2009.

[16] R. J. Mailloux, *Phased Array Antenna Handbook*. Norwood, MA, USA: Artech House, Nov. 2017.

[17] A. Ishimaru, "Theory of unequally-spaced arrays," *IRE Trans. Antennas Propag.*, vol. 10, no. 6, pp. 691–702, Nov. 1962.

[18] K. C. Kerby and J. T. Bernhard, "Sidelobe level and wideband behavior of arrays of random subarrays," *IEEE Trans. Antennas Propag.*, vol. 54, no. 8, pp. 2253–2262, Aug. 2006.

[19] N. Jin and Y. Rahmat-Samii, "Advances in particle swarm optimization for antenna designs: Real-number, binary, single-objective and multiobjective implementations," *IEEE Trans. Antennas Propag.*, vol. 55, no. 3, pp. 556–567, Mar. 2007.

[20] J. A. Nanzer, "Spatial filtering of grating lobes in mobile sparse arrays," in *Proc. IEEE Radio Wireless Symp.*, Jan. 2016, pp. 26–28.

[21] J. A. Nanzer, R. L. Schmid, T. M. Comberiate, and J. E. Hodkin, "Open-loop coherent distributed arrays," *IEEE Trans. Microw. Theory Techn.*, vol. 65, no. 5, pp. 1662–1672, May 2017.

[22] C. Pon, "Retrodirective array using the heterodyne technique," *IEEE Trans. Antennas Propag.*, vol. AP-12, no. 2, pp. 176–180, Mar. 1964.

[23] P. Bidigare *et al.*, "Implementation and demonstration of receiver-coordinated distributed transmit beamforming across an ad-hoc radio network," in *Proc. Conf. Rec. 46th Asilomar Conf. Signals, Syst. Comput. (ASILOMAR)*, Nov. 2012, pp. 222–226.

[24] R. Mudumbai, B. Wild, U. Madhow, and K. Ramchandran, "Distributed beamforming using 1 bit feedback: From concept to realization," in *Proc. 44th Allerton Conf. Commun., Control Comput.*, vol. 8, 2006, pp. 1020–1027.

[25] D. R. Brown and H. V. Poor, "Time-slotted round-trip carrier synchronization for distributed beamforming," *IEEE Trans. Signal Process.*, vol. 56, no. 11, pp. 5630–5643, Nov. 2008.

[26] R. D. Preuss and D. R. Brown, "Two-way synchronization for coordinated multicell retrodirective downlink beamforming," *IEEE Trans. Signal Process.*, vol. 59, no. 11, pp. 5415–5427, Nov. 2011.

[27] B. Peiffer, R. Mudumbai, S. Goguri, A. Kruger, and S. Dasgupta, "Experimental demonstration of retrodirective beamforming from a fully wireless distributed array," in *Proc. MILCOM IEEE Mil. Commun. Conf.*, Nov. 2016, pp. 442–447.

[28] I. Krikidis, "Retrodirective large antenna energy beamforming in backscatter multi-user networks," *IEEE Wireless Commun. Lett.*, vol. 7, no. 4, pp. 678–681, Aug. 2018.

[29] R. D. Preuss and D. R. Brown, "Retrodirective distributed transmit beamforming with two-way source synchronization," in *Proc. 44th Annu. Conf. Inf. Sci. Syst. (CISS)*, Mar. 2010, pp. 1–6.

[30] B. Khoshnevis, W. Yu, and R. Adve, "Grassmannian beamforming for MIMO amplify-and-forward relaying," *IEEE J. Sel. Areas Commun.*, vol. 26, no. 8, pp. 1397–1407, Oct. 2008.

[31] J. Joung and A. H. Sayed, "Multiuser two-way amplify-and-forward relay processing and power control methods for beamforming systems," *IEEE Trans. Signal Process.*, vol. 58, no. 3, pp. 1833–1846, Mar. 2010.

[32] K. Zarifi, S. Zaidi, S. Affes, and A. Ghrayeb, "A distributed amplify-and-forward beamforming technique in wireless sensor networks," *IEEE Trans. Signal Process.*, vol. 59, no. 8, pp. 3657–3674, Aug. 2011.

[33] F. Quitin, A. Irish, and U. Madhow, "Distributed receive beamforming: A scalable architecture and its proof of concept," in *Proc. IEEE 77th Veh. Technol. Conf. (VTC Spring)*, Jun. 2013, pp. 1–5.

[34] F. Quitin, A. T. Irish, and U. Madhow, "A scalable architecture for distributed receive beamforming: Analysis and experimental demonstration," *IEEE Trans. Wireless Commun.*, vol. 15, no. 3, pp. 2039–2053, Mar. 2016.

[35] D. R. Brown III, U. Madhow, M. Ni, M. Rebholz, and P. Bidigare, "Distributed reception with hard decision exchanges," *IEEE Trans. Wireless Commun.*, vol. 13, no. 6, pp. 3406–3418, Jun. 2014.

[36] J. Choi, D. J. Love, D. R. Brown, and M. Boutin, "Quantized distributed reception for MIMO wireless systems using spatial multiplexing," *IEEE Trans. Signal Process.*, vol. 63, no. 13, pp. 3537–3548, Jul. 2015.

[37] J. Choi, D. J. Love, and T. P. Bidigare, "Coded distributed diversity: A novel distributed reception technique for wireless communication systems," *IEEE Trans. Signal Process.*, vol. 63, no. 5, pp. 1310–1321, Mar. 2015.

[38] J.-J. van de Beek, O. Edfors, M. Sandell, S. K. Wilson, and P. O. Borjesson, "On channel estimation in OFDM systems," in *Proc. IEEE 45th Veh. Technol. Conf.*, vol. 2. Jul. 1995, pp. 815–819.

[39] O. Edfors, M. Sandell, J.-J. van de Beek, S. K. Wilson, and P. O. Borjesson, "OFDM channel estimation by singular value decomposition," *IEEE Trans. Commun.*, vol. 46, no. 7, pp. 931–939, Jul. 1998.

[40] S. Coleri, M. Ergen, A. Puri, and A. Bahai, "Channel estimation techniques based on pilot arrangement in OFDM systems," *IEEE Trans. Broadcast.*, vol. 48, no. 3, pp. 223–229, Sep. 2002.

[41] P. Chatterjee and J. A. Nanzer, "Effects of time alignment errors in coherent distributed radar," in *Proc. IEEE Radar Conf. (RadarConf)*, Apr. 2018, pp. 0727–0731.

[42] S. Mghabghab and J. A. Nanzer, "Ranging requirements for open-loop coherent distributed arrays with wireless frequency synchronization," in *Proc. IEEE USNC-CNC-URSI North Amer. Radio Sci. Meeting (Joint With AP-S Symp.)*, Jul. 2020, pp. 69–70.

[43] C. P. Mathews and M. D. Zoltowski, "Eigenstructure techniques for 2-D angle estimation with uniform circular arrays," *IEEE Trans. Signal Process.*, vol. 42, no. 9, pp. 2395–2407, Sep. 1994.

[44] M. D. Zoltowski and C. P. Mathews, "Real-time frequency and 2-D angle estimation with sub-Nyquist Spatio-temporal sampling," *IEEE Trans. Signal Process.*, vol. 42, no. 10, pp. 2781–2794, Oct. 1994.

[45] N. Tayem and H. M. Kwon, "L-shape 2-dimensional arrival angle estimation with propagator method," *IEEE Trans. Antennas Propag.*, vol. 53, no. 5, pp. 1622–1630, May 2005.

[46] A. Schlegel, S. M. Ellison, and J. A. Nanzer, "A microwave sensor with submillimeter range accuracy using spectrally sparse signals," *IEEE Microw. Wireless Compon. Lett.*, vol. 30, no. 1, pp. 120–123, Jan. 2020.

[47] S. Taylor, "High-precision tracking: An essential component of the optical multiple access (OMA) system," in *IEE Colloquium on Opt. Inter-satellite Links and on-Board Techn.* Edison, NJ, USA: IET, Jan. 1990, pp. 1–12.

[48] L. Hu, S. Zhang, and G. Lu, "Observation-to-track pairing using electro-optical(EO) systems," in *Proc. Int. Conf. Mechatronics Autom.*, Jun. 2006, pp. 589–594.

[49] A. Weiss and E. Weinstein, "Fundamental limitations in passive time delay estimation—Part I: Narrow-band systems," *IEEE Trans. Acoust., Speech, Signal Process.*, vol. ASSP-31, no. 2, pp. 472–486, Apr. 1983.

[50] E. Weinstein and A. Weiss, "Fundamental limitations in passive time-delay estimation—Part II: Wide-band systems," *IEEE Trans. Acoust., Speech, Signal Process.*, vol. ASSP-32, no. 5, pp. 1064–1078, Oct. 1984.

[51] J. A. Nanzer and M. D. Sharp, "On the estimation of angle rate in radar," *IEEE Trans. Antennas Propag.*, vol. 65, no. 3, pp. 1339–1348, Dec. 2016.

[52] J. E. Hodkin *et al.*, "Microwave and millimeter-wave ranging for coherent distributed RF systems," in *Proc. IEEE Aerosp. Conf.*, Mar. 2015, pp. 1–7.

[53] S. M. Ellison, S. Mghabghab, J. J. Doroshewitz, and J. A. Nanzer, "Combined wireless ranging and frequency transfer for internode coordination in open-loop coherent distributed antenna arrays," *IEEE Trans. Microw. Theory Techn.*, vol. 68, no. 1, pp. 277–287, Jan. 2020.

[54] S. M. Ellison and J. A. Nanzer, "High-accuracy multinode ranging for coherent distributed antenna arrays," *IEEE Trans. Aerosp. Electron. Syst.*, vol. 56, no. 5, pp. 4056–4066, Oct. 2020.

[55] A. Frischen, J. Hasch, and C. Waldschmidt, "A cooperative MIMO radar network using highly integrated FMCW radar sensors," *IEEE Trans. Microw. Theory Techn.*, vol. 65, no. 4, pp. 1355–1366, Apr. 2017.

[56] C. Pfeffer, R. Feger, C. Wagner, and A. Stelzer, "FMCW MIMO radar system for frequency-division multiple TX-beamforming," *IEEE Trans. Microw. Theory Techn.*, vol. 61, no. 12, pp. 4262–4274, Dec. 2013.

[57] B. Welp *et al.*, "Versatile dual-receiver 94-GHz FMCW radar system with high output power and 26-GHz tuning range for high distance applications," *IEEE Trans. Microw. Theory Techn.*, vol. 68, no. 3, pp. 1195–1211, Mar. 2020.

[58] S. Jeon *et al.*, "W-band MIMO FMCW radar system with simultaneous transmission of orthogonal waveforms for high-resolution imaging," *IEEE Trans. Microw. Theory Techn.*, vol. 66, no. 11, pp. 5051–5064, Nov. 2018.

[59] A. Stelzer, C. G. Diskus, K. Lubke, and H. W. Thim, "A microwave position sensor with submillimeter accuracy," *IEEE Trans. Microw. Theory Techn.*, vol. 47, no. 12, pp. 2621–2624, Dec. 1999.

[60] R. Feger, C. Wagner, S. Schuster, S. Scheiblhofer, H. Jager, and A. Stelzer, "A 77-GHz FMCW MIMO radar based on an SiGe single-chip transceiver," *IEEE Trans. Microw. Theory Techn.*, vol. 57, no. 5, pp. 1020–1035, May 2009.

[61] N. Pohl *et al.*, "Radar measurements with micrometer accuracy and nanometer stability using an ultra-wideband 80 GHz radar system," in *Proc. IEEE Topical Conf. Wireless Sensors Sensor Netw. (WiSNet)*, Jan. 2013, pp. 31–33.

[62] M. Morelli, C.-C.-J. Kuo, and M.-O. Pun, "Synchronization techniques for orthogonal frequency division multiple access (OFDMA): A tutorial review," *Proc. IEEE*, vol. 95, no. 7, pp. 1394–1427, Jul. 2007.
[63] M. Seo, M. Rodwell, and U. Madhow, "A feedback-based distributed phased array technique and its application to 60-GHz wireless sensor network," in *IEEE MTT-S Int. Microw. Symp. Dig.*, Jun. 2008, pp. 683–686.
[64] I. C. Sezgin *et al.*, "A low-complexity distributed-mimo testbed based on high-speed sigma-delta-over-fiber," *IEEE Trans. Microw. Theory Techn.*, vol. 67, no. 7, pp. 2861–2872, Apr. 2019.
[65] M. Ponton and A. Suarez, "Stability analysis of wireless coupled-oscillator circuits," in *IEEE MTT-S Int. Microw. Symp. Dig.*, Jun. 2017, pp. 83–86.
[66] X. Yang, X. Lu, and A. Babakhani, "Picosecond wireless synchronization using an optically locked voltage controlled oscillator (OL-VCO)," in *IEEE MTT-S Int. Microw. Symp. Dig.*, Jun. 2014, pp. 1–4.
[67] K.-Y. Tu and C.-S. Liao, "Application of ANFIS for frequency syntonization using GPS carrier-phase measurements," in *Proc. IEEE Int. Freq. Control Symp. Joint With 21st Eur. Freq. Time Forum*, May 2007, pp. 933–936.
[68] G. Barriac, R. Mudumbai, and U. Madhow, "Distributed beamforming for information transfer in sensor networks," in *Proc. 3rd Int. Symp. Inf. Process. Sensor Netw. (IPSN)*, Apr. 2004, pp. 81–88.
[69] D. R. Brown, G. B. Prince, and J. A. McNeill, "A method for carrier frequency and phase synchronization of two autonomous cooperative transmitters," in *Proc. IEEE 6th Workshop Signal Process. Adv. Wireless Commun.*, Jun. 2005, pp. 260–264.
[70] O. Abari, H. Rahul, D. Katabi, and M. Pant, "AirShare: Distributed coherent transmission made seamless," in *Proc. IEEE Conf. Comput. Commun. (INFOCOM)*, Apr. 2015, pp. 1742–1750.
[71] S. R. Mghabghab and J. A. Nanzer, "Open-loop distributed beamforming using wireless frequency synchronization," *IEEE Trans. Microw. Theory Techn.*, vol. 69, no. 1, pp. 896–905, Jan. 2021.
[72] S. M. Ellison, S. R. Mghabghab, and J. A. Nanzer, "Scalable high-accuracy ranging and wireless frequency synchronization for open-loop distributed phased arrays," in *Proc. IEEE 63rd Int. Midwest Symp. Circuits Syst. (MWSCAS)*, Aug. 2020, pp. 41–44.
[73] S. Mghabghab, H. Ouassal, and J. A. Nanzer, "Wireless frequency synchronization for coherent distributed antenna arrays," in *Proc. IEEE Int. Symp. Antennas Propag. USNC-URSI Radio Sci. Meeting*, Jul. 2019, pp. 1575–1576.
[74] H. Ouassal, T. Rocco, M. Yan, and J. A. Nanzer, "Decentralized frequency synchronization in distributed antenna arrays with quantized frequency states and directed communications," *IEEE Trans. Antennas Propag.*, vol. 68, no. 7, pp. 5280–5288, Jul. 2020.
[75] R. K. Pooler, J. S. Sunderlin, R. H. Tillman, and R. L. Schmid, "A precise RF time transfer method for coherent distributed system applications," in *Proc. USNC-URSI Radio Sci. Meeting (Joint With AP-S Symp.)*, Jul. 2018, pp. 5–6.
[76] F. Sivrikaya and B. Yener, "Time synchronization in sensor networks: A survey," *IEEE Netw.*, vol. 18, no. 4, pp. 45–50, Jul. 2004.
[77] S. Ganeriwal, R. Kumar, and M. B. Srivastava, "Timing-sync protocol for sensor networks," in *Proc. 1st Int. Conf. Embedded Netw. Sensor Syst. (SenSys)*, Nov. 2003, pp. 138–149.
[78] M. L. Sichitiu and C. Veerarittiphan, "Simple, accurate time synchronization for wireless sensor networks," in *Proc. IEEE Wireless Commun. Netw. Conf. (WCNC)*, vol. 2, Mar. 2003, pp. 1266–1273.
[79] D. R. Brown and A. G. Klein, "Precise timestamp-free network synchronization," in *Proc. 47th Annu. Conf. Inf. Sci. Syst. (CISS)*, Mar. 2013, pp. 1–6.
[80] M. Li, S. Gvozdenovic, A. Ryan, R. David, D. R. Brown, and A. G. Klein, "A real-time implementation of precise timestamp-free network synchronization," in *Proc. 49th Asilomar Conf. Signals, Syst. Comput.*, Nov. 2015, pp. 1214–1218.
[81] M. W. S. Overdick, J. E. Canfield, A. G. Klein, and D. R. Brown, "A software-defined radio implementation of timestamp-free network synchronization," in *Proc. IEEE Int. Conf. Acoust., Speech Signal Process. (ICASSP)*, Mar. 2017, pp. 1193–1197.
[82] F. Quitin, M. M. U. Rahman, R. Mudumbai, and U. Madhow, "A scalable architecture for distributed transmit beamforming with commodity radios: Design and proof of concept," *IEEE Trans. Wireless Commun.*, vol. 12, no. 3, pp. 1418–1428, Mar. 2013.
[83] T. M. Comberiate, K. S. Zilevu, J. E. Hodkin, and J. A. Nanzer, "Distributed transmit beamforming on mobile platforms using high-accuracy microwave wireless positioning," *Proc. SPIE*, vol. 9829, May 2016, Art. no. 98291S.

Jeffrey A. Nanzer (Senior Member, IEEE) received the B.S. degree in electrical engineering and computer engineering from Michigan State University, East Lansing, MI, USA, in 2003, and the M.S. and Ph.D. degrees in electrical engineering from The University of Texas at Austin, Austin, TX, USA, in 2005 and 2008, respectively.

From 2008 to 2009, he was a Post-Doctoral Fellow with the Applied Research Laboratories, The University of Texas at Austin, where he was involved in designing electrically small HF antennas and communication systems. From 2009 to 2016, he was with The Johns Hopkins University Applied Physics Laboratory, Laurel, MD, USA, where he created and led the Advanced Microwave and Millimeter-Wave Technology Section. In 2016, he joined the Department of Electrical and Computer Engineering, Michigan State University, where he is currently the Dennis P. Nyquist Assistant Professor. He has authored or coauthored more than 150 refereed journal articles and conference papers, authored *Microwave and Millimeter-Wave Remote Sensing for Security Applications* (Artech House, 2012), and coauthored the chapter "Photonics-Enabled Millimeter-Wave Wireless Systems" in *Wireless Transceiver Circuits* (Taylor & Francis, 2015). His current research interests include distributed arrays, radar and remote sensing, antennas, electromagnetics, and microwave photonics.

Dr. Nanzer was a founding member and the First Treasurer of the IEEE APS/MTT-S Central Texas Chapter. He is also a member of the IEEE Antennas and Propagation Society Education Committee and the USNC/URSI Commission B. He was a recipient of the Outstanding Young Engineer Award from the IEEE Microwave Theory and Techniques Society in 2019, the DARPA Director's Fellowship in 2019, the National Science Foundation (NSF) CAREER Award in 2018, the DARPA Young Faculty Award in 2017, and the JHU/APL Outstanding Professional Book Award in 2012. He has served as the Vice-Chair for the IEEE Antenna Standards Committee from 2013 to 2015 and the Chair of the Microwave Systems Technical Committee (MTT-16) of the IEEE Microwave Theory and Techniques Society from 2016 to 2018. He is also an Associate Editor of the IEEE TRANSACTIONS ON ANTENNAS AND PROPAGATION.

Serge R. Mghabghab (Graduate Student Member, IEEE) received the B.E. degree in electrical engineering from Notre Dame University—Louaize, Zouk Mosbeh, Lebanon, in 2014, and the M.E. degree in electrical and computer engineering from the American University of Beirut, Beirut, Lebanon, in 2017. He is currently pursuing the Ph.D. degree in electrical engineering at Michigan State University, East Lansing, MI, USA.

His current research interests include coherent distributed antenna arrays, radar and remote sensing, adaptive ranging, and wireless frequency synchronization.

Sean M. Ellison (Member, IEEE) received the B.S., M.S., and Ph.D. degrees in electrical and computer engineering from Michigan State University, East Lansing, MI, USA, in 2016, 2019, and 2020, respectively.

He is currently a Senior Professional Staff Member with the Radar and Electronic Warfare Systems Development Group, The Johns Hopkins University Applied Physics Laboratory (JHU/APL), Laurel MD, USA. His research interests include multistatic coherent radar technologies, signal processing, algorithm development, and waveform design for radar applications.

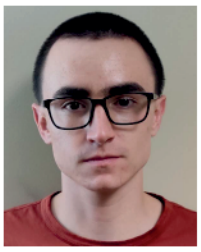

Anton Schlegel (Graduate Student Member, IEEE) received the B.S. degree in computer engineering from Michigan State University, East Lansing, MI, USA, in 2018, where he is currently pursuing the Ph.D. degree in electrical engineering.

His research interests include wireless microwave and millimeter-wave systems, distributed antenna arrays, and signal processing.